Electronic Supplementary Material (ESI) for Journal of Materials Chemistry C.

Supporting information for

Orthogonal Integration of Holographic and Fluorescent Dual Images based on Energy Transfer from Liquid Crystal to Photocleavable AIEgen

Ming Yao,[a] Ye Zhao,[a] Xingping Zhou,[a,b] Zhong'an Li,[a] Haiyan Peng,*[a,b] Xiaolin Xie[a,b]

[a] Key Lab for Material Chemistry of Energy Conversion and Storage, Ministry of Education, School of Chemistry and Chemical Engineering, Huazhong University of Science and Technology (HUST), Wuhan 430074, China

[b] National Anti-counterfeit Engineering Research Center, HUST, Wuhan 430074, China

E-mail: hypeng@hust.edu.cn (H. Y. Peng)

Synthesis of TPE-Cou

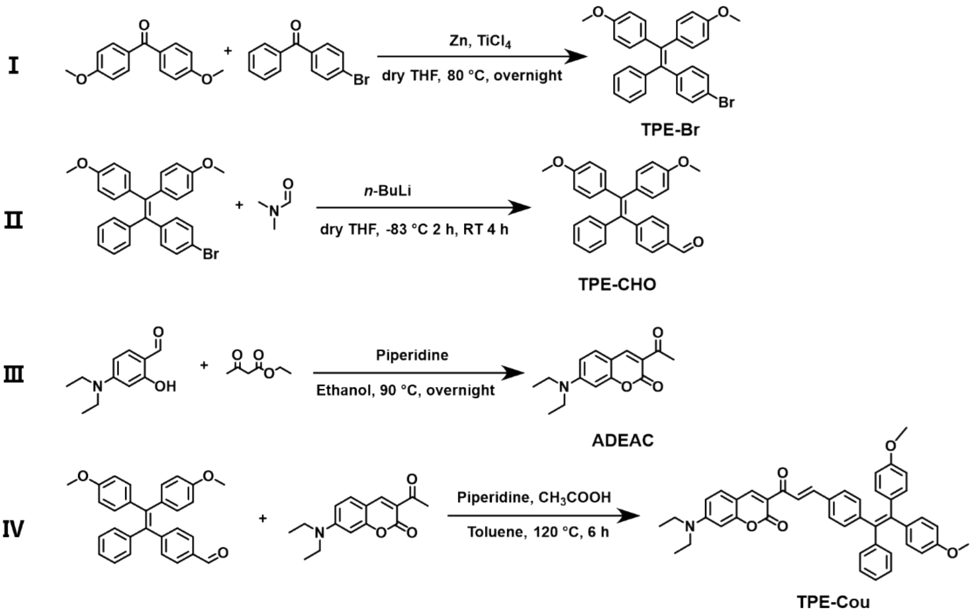

Scheme S1. Synthetic route to TPE-Cou

TPE-Cou was synthesized through a four-step method (**Scheme S1**):

(1) Synthesis of TPE-Br.[1] First, zinc powder (21.45 g, 328 mmol) and extra dry THF (100 mL) were added to a 500 mL Schlenk flask under argon atmosphere, and the system was cooled down to 0 °C. Subsequently, a solution of 4-bromobenzophenone (10.44 g, 40 mmol) and 4,4′-dimethoxybenzophenone (9.69 g, 40 mmol) in extra dry THF (200 mL) was added. Upon continuous stirring at 0 °C for 5 min, titanium tetrachloride (17.6 mL) was added dropwise at 0 °C, after which the system was slowly heated to room temperature, followed by refluxing at 80 °C for 12 h to complete the reaction. After cooling down to room temperature (RT), the mixture in flask was poured into water (1 L), extracted 3 times with ethyl acetate (100 mL for each extraction), further washed twice with brine (100 mL), and finally dried over Na_2SO_4. The residual oil phase was purified through column chromatography with mobile phase of *n*-hexane/ethyl acetate (200:1 in volume), and concentrated by rotatory evaporation,

yielding TPE-Br as a white solid (yield: 40%). ^{1}H NMR ($CDCl_3$, 400 MHz, **Fig. S1**, ESI), δ (ppm): 7.23-7.19 (d, J = 8.4 Hz, 2H), 7.14-7.08 (m, 3H), 7.03-6.98 (m, 2H), 6.96-6.85 (m, 6H), 6.69-6.60 (m, 4H), 3.76 (s, 3H), 3.73 (s, 3H).

(2) Synthesis of TPE-CHO.[1] 1.6 M *n*-butyllithium in hexane (8 mL) was added slowly to 50 mL extra dry THF solution of TPE-Br (3.02 g, 6.4 mmol) at −83 °C under argon atmosphere, followed by continuous stirring at the same temperature for 2 h. Then 3.5 mL (45 mmol) of extra dry DMF was added dropwise. The reaction mixture was warmed up to room temperature and kept stirring for another 4 h. Subsequently, the reaction was quenched by adding 10 mL saturated ammonium chloride aqueous solution, and then washed with 500 mL water, extracted three times with ethyl acetate (100 mL for each extraction), washed twice with brine (100 mL for each time). The organic phase was collected and dried over Na_2SO_4. After filtration, the crude product was purified by silica gel column chromatography with an eluent of *n*-hexane/ethyl acetate (60:1 in volume), yielding TPE-CHO as green solids (yield: 46%). ^{1}H NMR ($CDCl_3$, 400 MHz, **Fig. S2**, ESI), δ (ppm): 9.90 (s, 1H), 7.65-7.58 (d, J = 8.0 Hz, 2H), 7.21-7.16 (d, J = 8.0 Hz, 2H), 7.15-7.09 (m, 3H), 7.03-6.98 (m, 2H), 6.96-6.89 (m, 4H), 6.68-6.61 (d, J = 8.8 Hz, 4H), 3.75 (s, 6H).

(3) Synthesis of ADEAC.[2] 4-(Diethylamino)salicylaldehyde (5.30 g, 27 mmol), ethyl acetoacetate (35.74 g, 270 mmol) and 50 mL ethanol were added into a two-neck flask (100 mL), followed by dropping 1 mL piperidine. After refluxing at 90 °C overnight, the resulting yellow precipitate was collected by sequential filtration and washing with anhydrous ethanol, giving rise to yellow solids (yield: 76 %). ^{1}H NMR

($CDCl_3$, 400 MHz, **Fig. S3**, ESI), δ (ppm): 8.44 (s, 1H), 7.46-7.33 (d, *J* = 8.8 Hz, 1H), 6.67-6.58 (d, *J* = 8.8 Hz, 1H), 6.48 (s, 1H), 3.57-3.37 (m, 4H), 2.68 (s, 1H), 1.33-1.14 (m, 2H).

(4) Synthesis of TPE-Cou.[3] ADEAC (1.13 g, 4.0 mmol) and TPE-CHO (1.56 g, 3.8 mmol) were dissolved in 20 mL toluene, followed by dropping 1 mL piperidine and 1 mL acetic acid. Subsequently, the reaction mixture was warmed to 120 °C and refluxed for 6 h upon continuous stirring. After the reaction, the organic was extracted with ethyl acetate 3 times (100 mL for each) and washed with saline, then dried over anhydrous Na_2SO_4, filtered and concentrated under vacuum to yield the crude product. Further purification was conducted by silica gel column chromatography wherein the eluting phase was *n*-hexane/ethyl acetate (5:1 in volume). TPE-Cou was finally obtained as red solids with a reaction yield of 13%. ^1H NMR ($CDCl_3$, 400 MHz, **Fig. S4**, ESI), δ (ppm): 8.53 (s, 1H), 8.07-7.98 (d, *J* = 15.7 Hz, 1H), 7.78-7.70 (d, *J* = 15.7 Hz, 1H), 7.46-7.39 (m, 3H), 7.15-7.08 (m, 3H), 7.06-7.00 (m, 4H), 6.97-6.91 (m, 4H), 6.69-6.60 (m, 5H), 6.54-6.50 (d, *J* = 2.4 Hz, 1H), 3.77-3.72 (d, *J* = 6.4 Hz, 6H), 3.51-3.42 (m, 4H), 1.26-1.22 (m, 6H). ^{13}C NMR ($CDCl_3$, 100 MHz, **Fig. S5**, ESI), δ (ppm): 186.45, 160.88, 158.66, 158.39, 158.20, 152.94, 148.61, 146.84, 143.94, 143.27, 141.15, 138.61, 136.15, 136.02, 133.08, 132.63, 131.83, 131.78, 131.45, 128.26, 127.81, 126.28, 124.29, 116.90, 113.21, 113.01, 109.88, 108.68, 96.68, 55.11, 55.09, 45.19, 12.49. High resolution mass spectrometry (HRMS) (positive scan, m/z, **Fig. S6**, ESI): calculated for $[M + H]^+$, 662.6907; found, 662.6895.

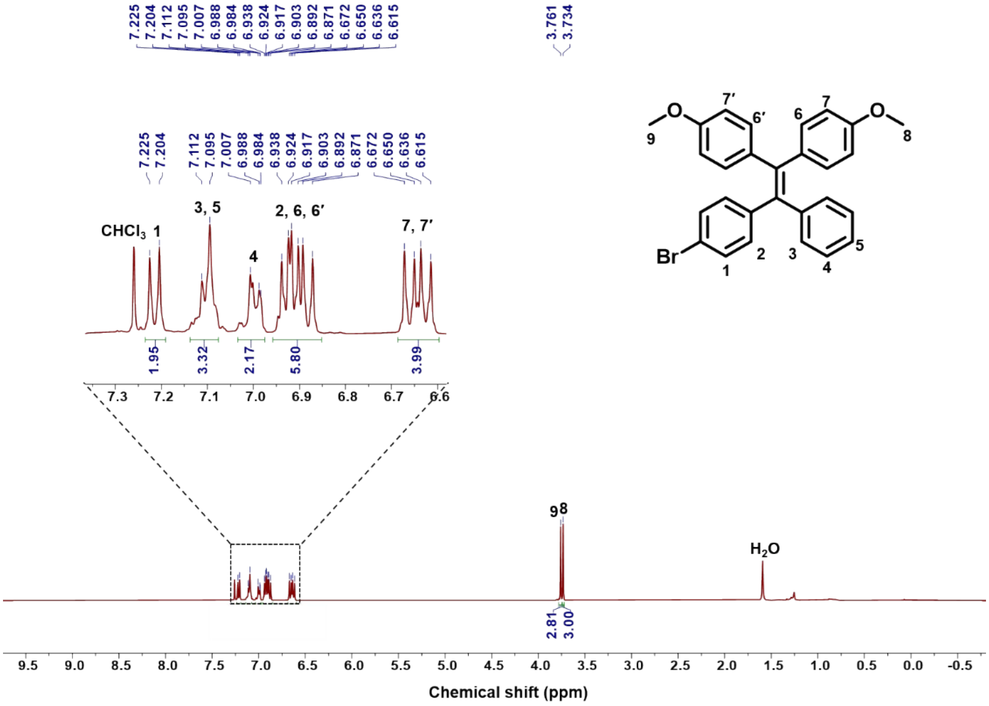

Fig. S1 ^{1}H-Nuclear magnetic resonance (NMR) spectrum of 4,4'-(2-(4-bromophenyl)-2-phenylethene-1,1-diyl) bis(methoxybenzene), *i.e.*, TPE-Br in $CDCl_3$.

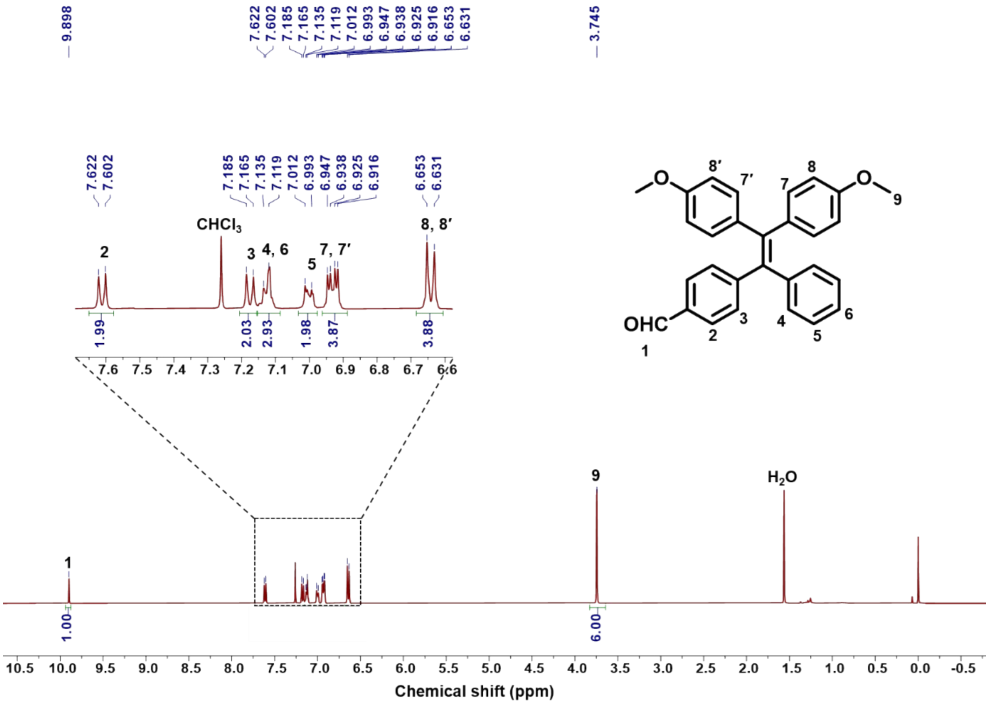

Fig. S2 ^{1}H-NMR spectrum of 4-(2,2-bis(4-methoxyphenyl)-1-phenylvinyl) benzaldehyde, *i.e.*, TPE-CHO in $CDCl_3$.

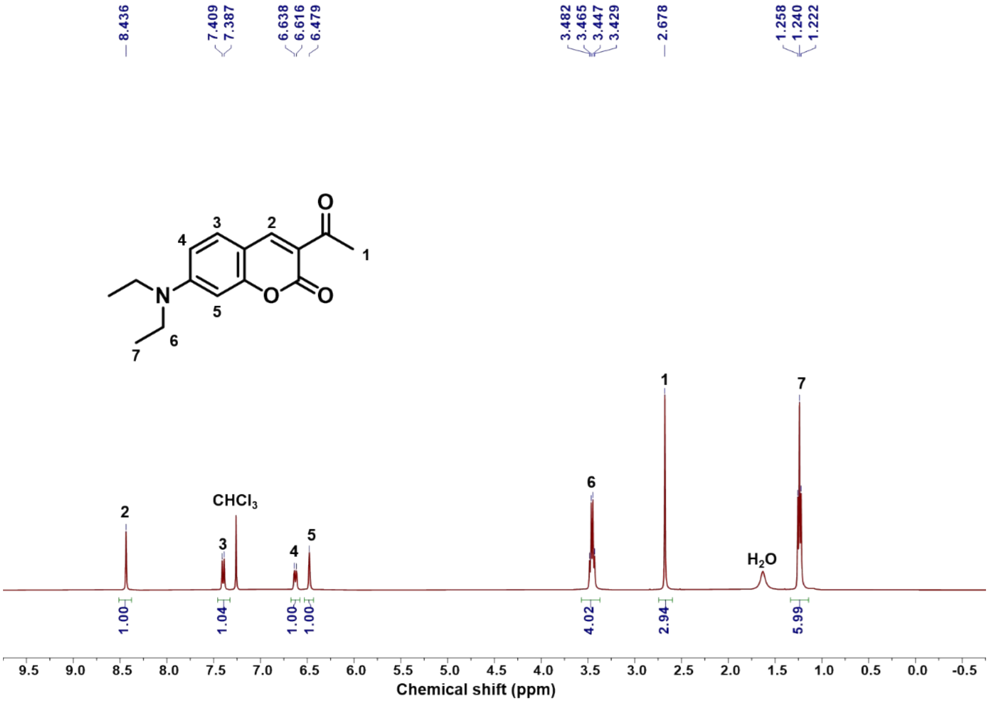

Fig. S3 ^{1}H-NMR spectrum of 3-acetyl-7-diethylaminocoumarin, *i.e.*, ADEAC in $CDCl_3$.

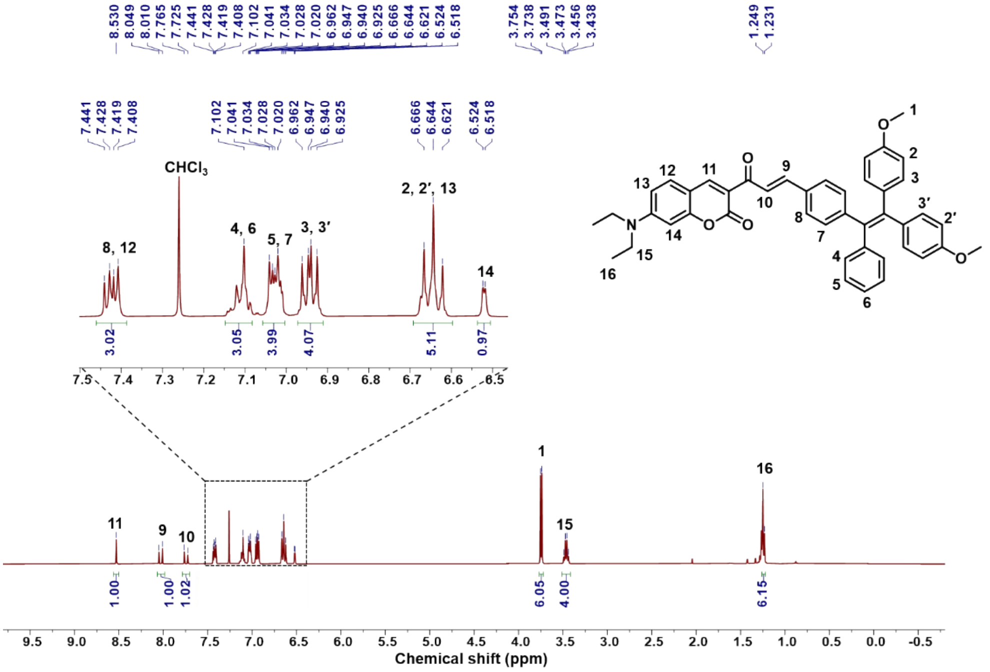

Fig. S4 ^{1}H-NMR spectrum of 3-(3-(4-(2,2-bis(4-methoxyphenyl)-1-phenylvinyl)phenyl)acryloyl)-7-diethylamino-2*H*-chromen-2-one, i.e., TPE-Cou in $CDCl_3$.

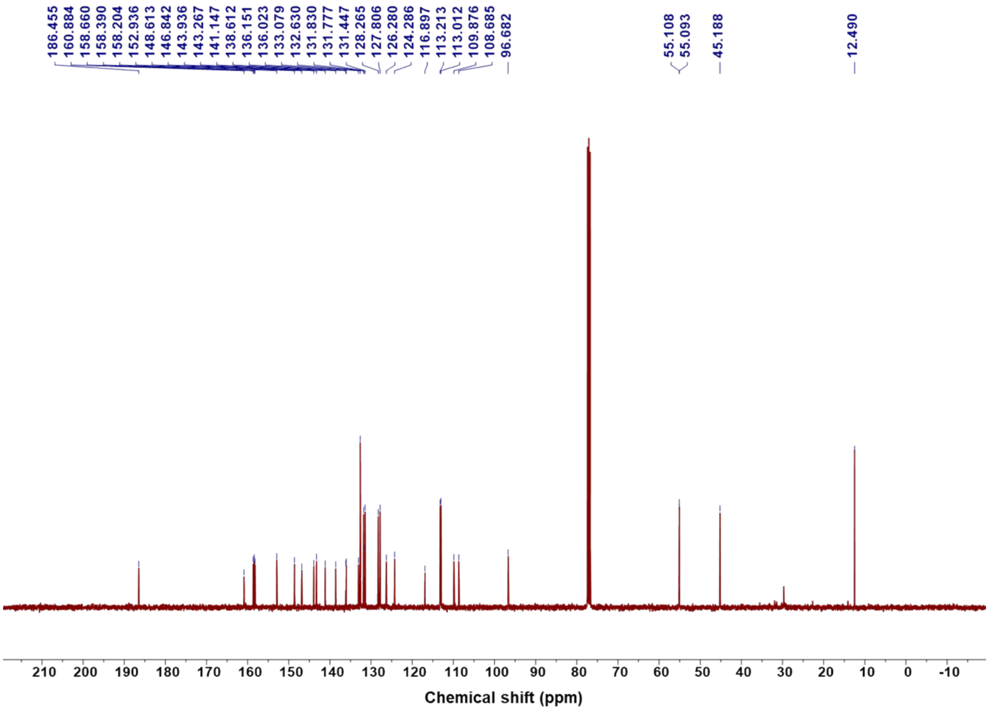

Fig. S5 ^{13}C-NMR spectrum of TPE-Cou in $CDCl_3$.

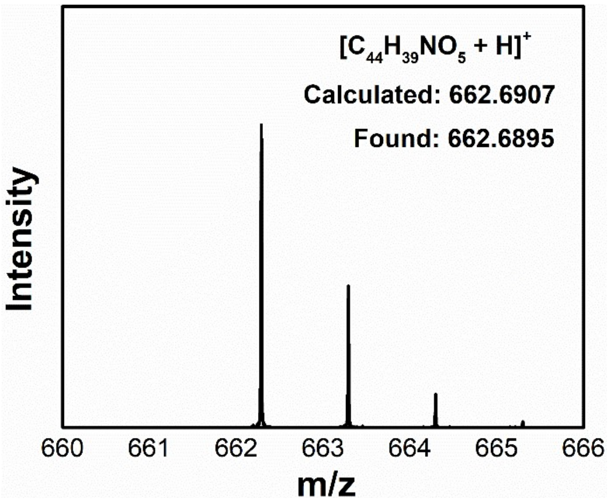

Fig. S6 HRMS of TPE-Cou.

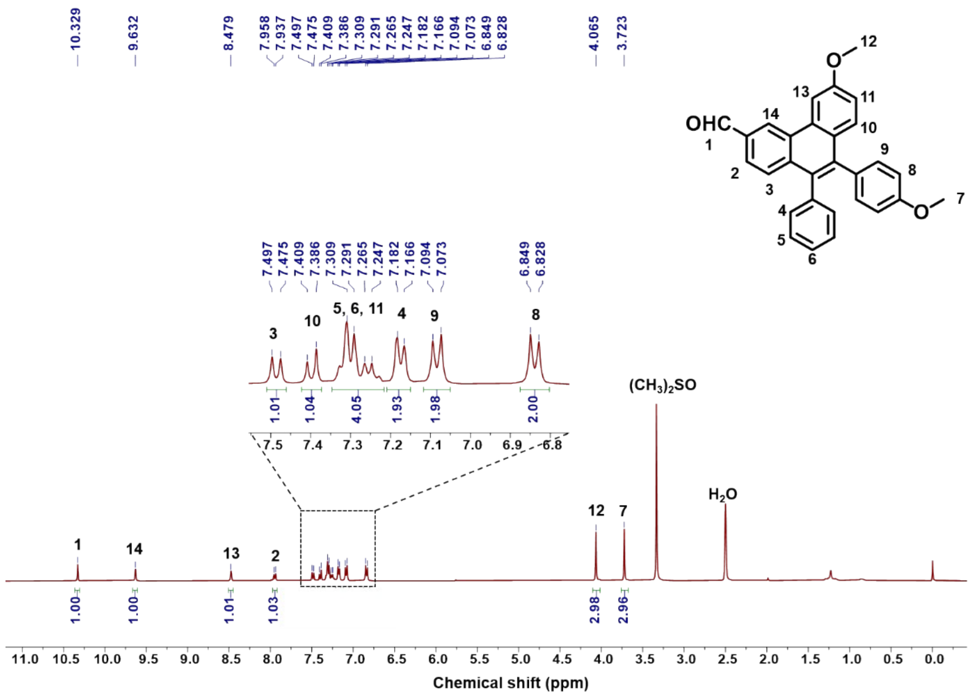

Fig. S7 ^{1}H-NMR spectrum of 6-methoxy-9-(4-methoxyphenyl)-10-phenylphenanthrene-3-carbaldehyde, *i.e.*, DPP-CHO in $CDCl_3$.

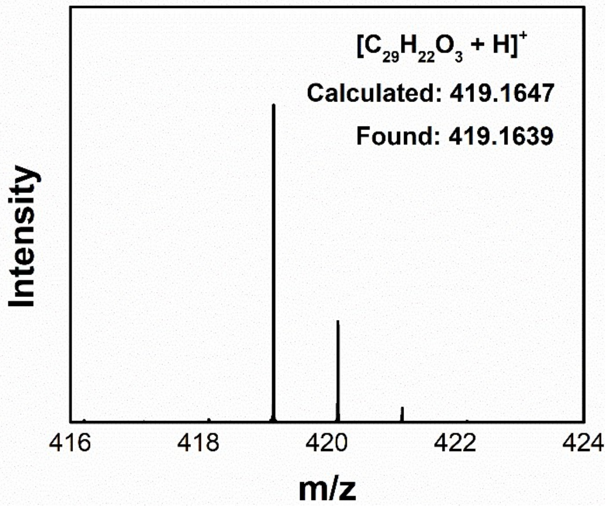

Fig. S8 HRMS of DPP-CHO.

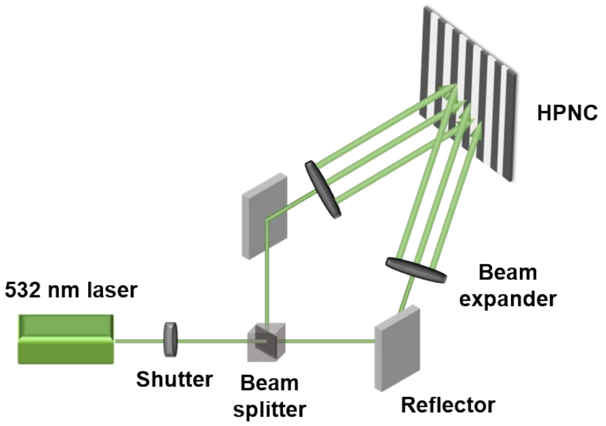

Fig. S9 Schematic of optical setups for holographic patterning.

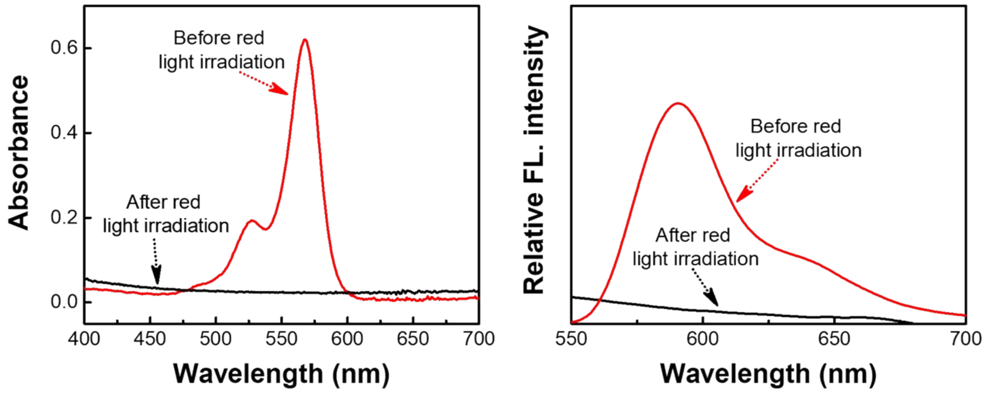

Fig. S10 (a) UV-vis absorption and (b) Fluorescence emission spectra of the polymer/P0616A composite film containing RB before and after red light irradiation for 100 h. Light intensity: 9 mW·cm^{-2}.

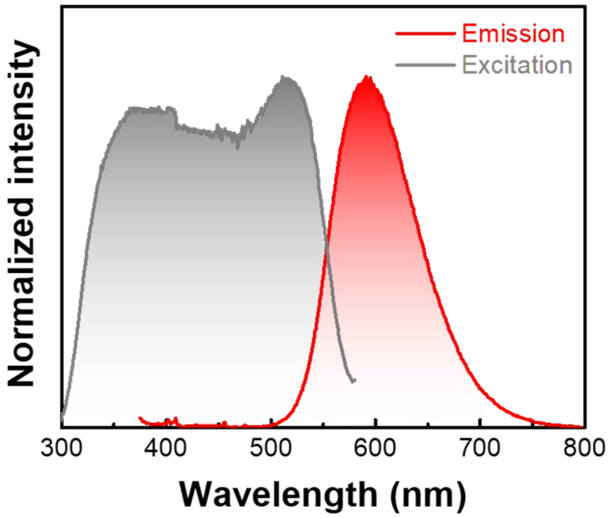

Fig. S11 Fluorescence emission (excitation@350 nm) and excitation spectrum (emission@591 nm) of TPE-Cou in bulk.

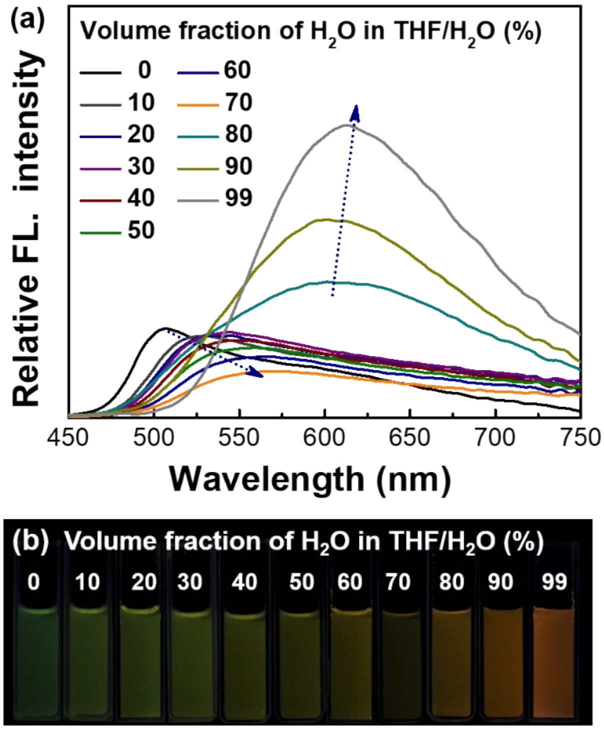

Fig. S12 (a) Fluorescence emission spectra of TPE-Cou in the THF/water mixture with varied volume fractions of water. (b) Fluorescent pictures of TPE-Cou in the mixture. Concentration of TPE-Cou: 10 μM. Excitation wavelength was 430 nm to eliminate side reactions.

Table S1 Formulations for holographic patterning

Entry	Monomer (wt%)[a]	LC[b] (wt%)	TPE-Cou (wt%)	Weight ratio of TPE-Cou to LC	RB[c]	NPG[c]
1	67.0	33.0	0.0	0.00	1.0	1.3
2		32.4	0.6	0.02		
3		31.7	1.3	0.04		
4		31.1	1.9	0.06		
5		30.6	2.4	0.08		
6		30.0	3.0	0.10		
7		29.5	3.5	0.12		
8		28.9	4.1	0.14		

[a] The monomer consists of DMAA and 6361-100 (2:1 by weight)[4,5]

[b] LC was P0616A in this work

[c] Ratio to the total mass of the monomer, LC and TPE-Cou

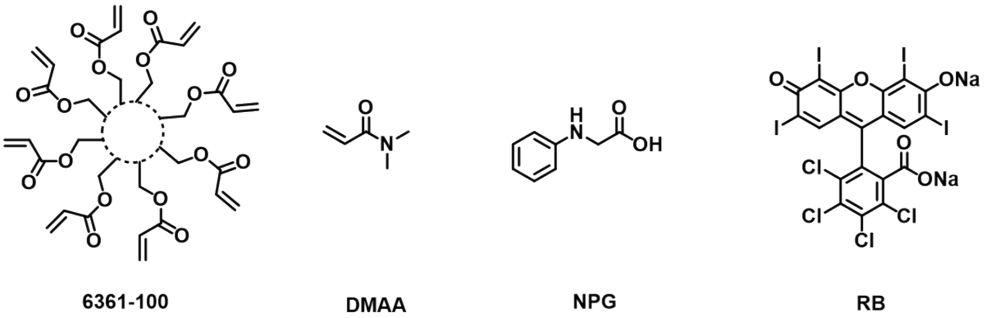

Fig. S13 Chemical structures of 6361-100, DMAA, NPG and RB.

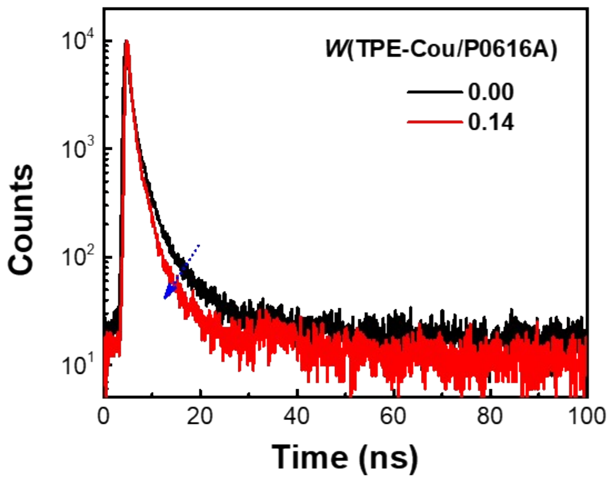

Fig. S14 Time-dependent fluorescent decay of polymer/P0616A/TPE-Cou composites at 385 nm. Excitation wavelength: 375 nm.

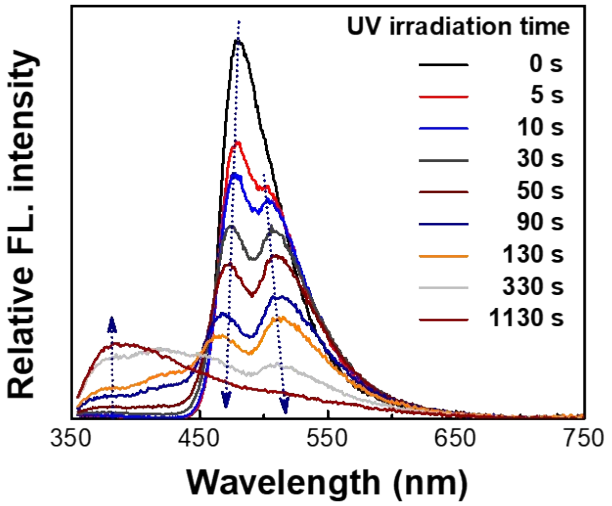

Fig. S15 Fluorescence change of the polymer/P0616A/ADEAC composite film upon UV irradiation. The weight ratio of the ADEAC to P0616A was 0.05. UV irradiation wavelength: 365 nm, intensity: 90 mW·cm^{-2}. The chemical structure of ADEAC is displayed in **Fig. S3**.

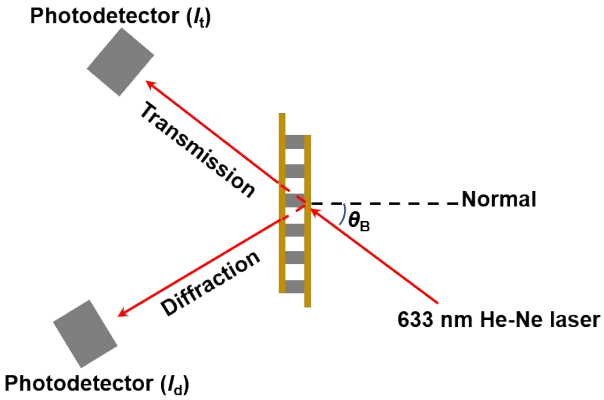

Fig. S16 Schematic illustration of diffraction efficiency (η) characterization. Diffraction efficiency was defined as the intensity ratio of diffraction to the sum of diffraction and transmission at the Bragg angle (θ_B). The Bragg angle is the specific incident angle at which the Bragg condition is satisfied, and η reaches the maximum. The total intensity of the probe laser is 4 mW·cm^{-2}.

$$\eta = \frac{I_d}{I_t + I_d} \times 100\%$$

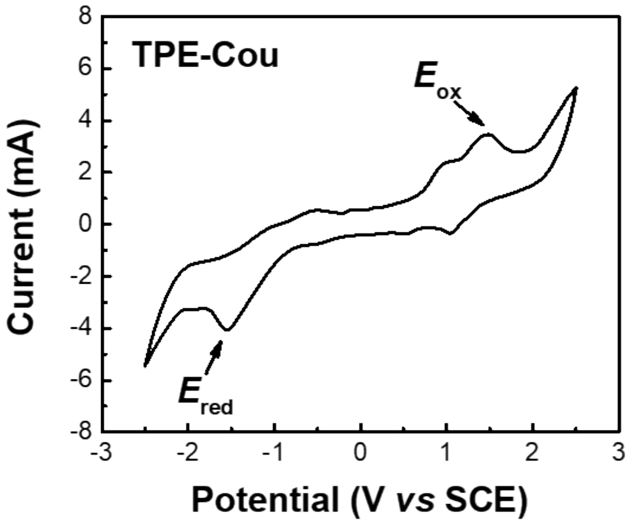

Fig. S17 Cyclic voltammetry (CV) curve of TPE-Cou in acetonitrile. TPE-Cou concentration: 1 mM; CV scanning rate: 1.0 V·s^{-1}. SCE stands for standard calomel electrode.

Table S2 Redox potentials of RB, NPG and TPE-Cou, respectively

Chemical	E_{ox} (V *vs* SCE)	E_{red} (V *vs* SCE)	Triplet energy (E_T, eV)
RB[a]	+0.65	–1.00	+1.80
NPG[a]	+0.42	/	/
TPE-Cou	+1.49	–1.56	+1.68[b]

[a] The value is given by reference[6]

[b] The value is calculated by the DFT method

When considering electron transfer from TPE-Cou to the triplet RB,

$$\Delta G = e[E_{ox}\ (\text{TPE-Cou}) - E_{red}\ (\text{RB})] - E_T\ (\text{RB})$$

$$= +1.49\ \text{eV} - (-1.00\ \text{eV}) - 1.80\ \text{eV} = +0.69\ \text{eV} > 0$$

When considering electron transfer from the triplet RB to TPE-Cou,

$$\Delta G = e[E_{ox}\ (\text{RB}) - E_{red}\ (\text{TPE-Cou})] - E_T\ (\text{RB})$$

$$= +0.65\ \text{eV} - (-1.56\ \text{eV}) - 1.80\ \text{eV} = +0.41\ \text{eV} > 0$$

When considering electron transfer from NPG to the triplet TPE-Cou,

$$\Delta G = e[E_{ox}\ (\text{NPG}) - E_{red}\ (\text{TPE-Cou})] - E_T\ (\text{TPE-Cou})$$

$$= +0.42\ \text{eV} - (-1.56\ \text{eV}) - 1.68\ \text{eV} = +0.30\ \text{eV} > 0$$

Minimum Energy Geometry Optimized at the M06-2X/6311G(d,p) Level

Table S3 Cartesian coordinates of the optimized triplet structure of TPE-Cou

Center number	**Atomic number**	**Cartesian coordinates/Angstroms**		
		X	**Y**	**Z**
1	6	-10.2172	0.02676	-1.32658
2	6	-10.3452	-0.24965	0.0645
3	6	-9.17388	-0.37618	0.83282
4	6	-7.93906	-0.23056	0.22681
5	6	-7.80116	0.04291	-1.13979
6	6	-8.97748	0.16674	-1.89839
7	8	-6.84577	-0.36496	1.01249
8	6	-5.53945	-0.24791	0.55668
9	6	-5.3779	0.04127	-0.87335
10	6	-6.48326	0.17515	-1.65339
11	8	-4.68555	-0.39436	1.38371
12	7	-11.5752	-0.38911	0.63861
13	6	-12.7757	-0.29337	-0.16999
14	6	-11.6783	-0.66446	2.05887
15	6	-4.04287	0.21046	-1.55108
16	6	-2.79383	0.0344	-0.7802
17	8	-4.02849	0.4871	-2.73657
18	6	-1.61256	0.20444	-1.39848
19	6	-0.29698	0.06556	-0.79451
20	6	0.8475	0.20686	-1.59611
21	6	2.11622	0.07304	-1.07245
22	6	2.31382	-0.24603	0.29306
23	6	1.15215	-0.34486	1.10524
24	6	-0.10827	-0.19247	0.5767
25	6	3.64013	-0.38708	0.81822
26	6	4.77752	0.19889	0.05499
27	6	5.68656	-0.71201	-0.60575
28	6	7.03372	-0.37908	-0.88698
29	6	7.88681	-1.27794	-1.48803
30	6	7.44053	-2.55794	-1.83691
31	6	6.12564	-2.92569	-1.54833

32	6	5.27588	-2.01728	-0.93381
33	6	3.94727	-1.09292	2.05468
34	6	5.09955	-0.75932	2.7934
35	6	5.42067	-1.43669	3.9587
36	6	4.62189	-2.48582	4.40749
37	6	3.50187	-2.85754	3.669
38	6	3.16818	-2.17517	2.50969
39	6	4.89995	1.63928	0.0172
40	6	5.55182	2.32468	-1.0369
41	6	5.61705	3.70011	-1.06923
42	6	5.03336	4.46457	-0.0521
43	6	4.36214	3.81967	0.98796
44	6	4.29172	2.43428	1.0069
45	8	5.15683	5.8085	-0.17488
46	6	4.54893	6.61538	0.81203
47	8	8.35527	-3.36447	-2.42857
48	6	7.95058	-4.67359	-2.77015
49	1	-11.0974	0.12968	-1.94388
50	1	-9.19193	-0.58875	1.89123
51	1	-8.89298	0.37827	-2.95864
52	1	-6.32892	0.39182	-2.70634
53	1	-12.8751	0.69629	-0.62781
54	1	-12.7848	-1.04615	-0.96508
55	1	-11.2068	-1.61877	2.3177
56	1	-11.2044	0.12564	2.65012
57	1	-2.87331	-0.23103	0.26249
58	1	-1.63852	0.46411	-2.45444
59	1	0.72336	0.42627	-2.65122
60	1	2.98034	0.19097	-1.71646
61	1	1.26311	-0.50172	2.17068
62	1	-0.96607	-0.25368	1.23592
63	1	7.41638	0.58824	-0.58606
64	1	8.92143	-1.0271	-1.68771
65	1	5.75443	-3.91212	-1.79108
66	1	4.25841	-2.3214	-0.71218
67	1	5.7348	0.04763	2.44404

68	1	6.30375	-1.15104	4.51809
69	1	4.87962	-3.01957	5.31416
70	1	2.89232	-3.69379	3.99082
71	1	2.31801	-2.50174	1.92329
72	1	5.9722	1.76026	-1.85994
73	1	6.10072	4.22185	-1.88598
74	1	3.88533	4.38114	1.77997
75	1	3.75723	1.94965	1.81707
76	1	4.75289	7.6448	0.52677
77	1	3.46688	6.45336	0.84407
78	1	4.97621	6.42105	1.80112
79	1	8.81734	-5.14761	-3.22466
80	1	7.64944	-5.23896	-1.88244
81	1	7.1255	-4.65811	-3.48943
82	1	-13.643	-0.46155	0.46402
83	1	-12.7282	-0.71405	2.33742

Table S4 Cartesian coordinates of the optimized singlet structure of TPE-Cou

Center number	**Atomic number**	**Cartesian coordinates/Angstroms**		
		X	**Y**	**Z**
1	6	-10.32934	0.48373	-0.67466
2	6	-10.3714	-0.49096	0.36309
3	6	-9.15496	-0.98815	0.8652
4	6	-7.95999	-0.52628	0.34364
5	6	-7.90664	0.43095	-0.67742
6	6	-9.12756	0.92232	-1.17088
7	8	-6.82081	-1.0394	0.86235
8	6	-5.54486	-0.68328	0.44588
9	6	-5.47228	0.31882	-0.62407
10	6	-6.62334	0.83051	-1.13567
11	8	-4.64119	-1.23234	1.0081
12	7	-11.56381	-0.93233	0.85747
13	6	-12.8119	-0.41144	0.33233
14	6	-11.58038	-1.92225	1.91755
15	6	-4.18293	0.83206	-1.20914

16	6	-2.88458	0.29788	-0.73568
17	8	-4.243	1.68341	-2.07616
18	6	-1.75491	0.7626	-1.28707
19	6	-0.3886	0.35784	-0.95707
20	6	0.67641	0.95411	-1.64202
21	6	1.99032	0.60986	-1.3668
22	6	2.28574	-0.34668	-0.39212
23	6	1.2197	-0.96493	0.27637
24	6	-0.09144	-0.61246	0.00981
25	6	3.69003	-0.74177	-0.09316
26	6	4.68161	0.16613	0.08635
27	6	6.11712	-0.22212	0.14422
28	6	6.95843	0.30617	1.1334
29	6	8.28968	-0.05624	1.20752
30	6	8.82836	-0.94451	0.27191
31	6	8.01585	-1.45649	-0.73845
32	6	6.67432	-1.09155	-0.7908
33	6	3.92378	-2.21301	-0.01217
34	6	4.65231	-2.77504	1.04061
35	6	4.85999	-4.14624	1.10541
36	6	4.34236	-4.98057	0.11927
37	6	3.60246	-4.43479	-0.92401
38	6	3.3862	-3.06341	-0.98304
39	6	4.41517	1.62259	0.23683
40	6	5.19528	2.56154	-0.45297
41	6	4.94755	3.9163	-0.34239
42	6	3.92006	4.37676	0.4859
43	6	3.15446	3.46103	1.20643
44	6	3.40997	2.0997	1.07505
45	8	3.75334	5.72201	0.53009
46	6	2.70844	6.22673	1.335
47	8	10.14444	-1.23765	0.42344
48	6	10.72667	-2.13254	-0.50032
49	1	-11.24616	0.88553	-1.0803
50	1	-9.10778	-1.72597	1.65211
51	1	-9.10797	1.66373	-1.96212

52	1	-6.53337	1.57138	-1.92469
53	1	-12.89394	0.66937	0.48758
54	1	-12.91341	-0.61706	-0.73818
55	1	-11.09223	-2.85062	1.60291
56	1	-11.07362	-1.55348	2.81559
57	1	-2.89502	-0.45179	0.04055
58	1	-1.85956	1.51956	-2.06121
59	1	0.46419	1.69643	-2.4041
60	1	2.80089	1.08754	-1.90501
61	1	1.43218	-1.72771	1.01761
62	1	-0.89302	-1.09942	0.55271
63	1	6.55191	1.00591	1.85584
64	1	8.94383	0.33603	1.97616
65	1	8.40795	-2.13376	-1.48486
66	1	6.04627	-1.49893	-1.57481
67	1	5.06185	-2.12532	1.80563
68	1	5.42494	-4.56527	1.92973
69	1	4.50664	-6.05038	0.16924
70	1	3.18864	-5.07849	-1.69125
71	1	2.79896	-2.64015	-1.79105
72	1	6.00056	2.21493	-1.0915
73	1	5.53525	4.64723	-0.88357
74	1	2.36436	3.78801	1.86824
75	1	2.80707	1.39396	1.63515
76	1	2.73276	7.30748	1.21628
77	1	1.73623	5.84573	1.00652
78	1	2.86179	5.97377	2.38904
79	1	11.76839	-2.23453	-0.2051
80	1	10.23963	-3.11243	-0.46325
81	1	10.67487	-1.73915	-1.52064
82	1	-12.61164	-2.15015	2.17636
83	1	-13.64008	-0.89152	0.84822

Notes and References

1. Y. Y. Yuan, C. J. Zhang, M. Gao, R. Y. Zhang, B. Z. Tang and B. Liu, *Angew. Chem., Int. Ed.*, 2015, **54**, 1780.
2. L. L. Long, Y. Y. Han, W. G. Liu, Q. Chen, D. D. Yin, L. L. Li, F. Yuan, Z. X. Han, A. H. Gong and K. Wang, *Anal. Chem.*, 2020, **92**, 6072.
3. Y. K. Yue, F. J. Huo, P. Yue, X. M. Meng, J. C. Salamanca, J. O. Escobedo, R. M. Strongin and C. X. Yin, *Anal. Chem.*, 2018, **90**, 7018.
4. X. M. Zhang, W. J. Yao, X. P. Zhou, W. Wei, Q. K. Liu, H. Y. Peng, J. T. Zhu, I. I. Smalyukh and X. L. Xie, *Compos. Sci. Technol.*, 2019, **181**, 107705.
5. W. Luo, M. L. Ni, X. P. Zhou, H. Y. Peng and X. L. Xie, *Compos. Part B: Eng.*, 2020, **199**, 108290.
6. G. N. Chen, M. L. Ni, H. Y. Peng, F. H. Huang, Y. G. Liao, M. K. Wang, J. T. Zhu, V. A. Roy and X. L. Xie, *ACS Appl. Mater. Interfaces*, 2017, **9**, 1810.